Chain conformation of polyacrylonitrile: a comparison of model scattering and radial distribution functions with experimental wide-angle X-ray scattering results

Johannes Ganster, Hans-Peter Fink* and Ingrid Zenke
Institut für Polymerenchemie 'Erich Correns', Kanststrasse 55, 1530 Teltow-Seehof, Germany
(Received 5 December 1989; revised 4 May 1990; accepted 26 June 1990)

Scattering and radial distribution functions were obtained for commercial polyacrylonitrile homopolymer in the solid state using wide-angle X-ray scattering. For three kinds of single chains with increasing conformational flexibility, namely (α) the planar zigzag chain, (β) a PCILO (perturbed configuration interaction with localized orbitals) chain based on quantum-chemical conformational energy calculations with the PCILO method and (γ) the restricted-rotation chain, model functions in real and reciprocal space have been calculated and compared with the experimental curves. While (α) can be ruled out, the experimental findings are intermediate between (β) and (γ) with a tendency to (γ). This suggests that energetically favourable single-chain conformations are somewhat distorted by interchain interactions.

(Keywords: polyacrylonitrile; chain conformation; radial distribution function; model calculations; wide-angle X-ray scattering)

INTRODUCTION

Since the classical X-ray work of Bohn, Schaefgen and Statton in 1961[1], the chain conformation of polyacrylonitrile (PAN) has been a topic of much attention (see e.g. ref. 2 and references cited therein). Although several attempts have been made, agreement about unit-cell dimensions or even space group has not been reached (see ref. 3 for a compilation of proposed unit-cell models). This is mainly due to the very limited number of spots in the diffraction pattern of PAN, which is again probably caused by the lack of stereoregularity in conventional (radically polymerized) PAN[4], thus hindering the growth of crystalline regions of sufficient order.

In the present work, the radial distribution function (RDF) method[5], a typical technique for the characterization of amorphous low-molecular-weight substances and amorphous polymers[6,7], has been applied to elucidate the chain conformation in solid commercial PAN homopolymer.

Scattering functions for three kinds of single-chain models with strongly different conformational characteristics have been calculated. The degree of conformational freedom is increased from (α), the planar zigzag conformation, via (β), a PCILO (perturbed configuration interaction with localized orbitals) chain based on quantum-chemical conformational energy calculations for acrylonitrile diads with the PCILO method, to (γ), a chain for which the internal rotation is only restricted by van der Waals hard-sphere repulsion of atoms (restricted-rotation chain).

Measurements have been performed on commercial PAN homopolymer powder (radically polymerized in solution) with Mo K_α radiation and for the first time RDFs for PAN have been calculated. Comparing model and experimental functions in real and reciprocal space, conclusions are drawn about the chain conformation of PAN in the solid state.

EXPERIMENTAL

Measurements have been performed on a commercial PAN homopolymer powder radically polymerized in solution (average molecular weight $\bar{M}_w = 1.2 \times 10^5$), using a horizontal diffractometer in symmetrical transmission geometry according to ref. 8. The incident Mo K_α radiation (wavelength $\lambda = 0.07107$ nm) was monochromatized by a flat LiF crystal and the diffracted beam (including Compton scattering) was detected by a scintillation counter, discriminating the $\lambda/2$ component by a pulse-height analyser. An aluminium frame of 3 mm thickness, covered by 12 μm thick polyester foils, was used as the sample holder.

Within 200 angular positions between Bragg angles of $\theta = 1°$ and 60.7° and with a step width of $\Delta\theta = 0.3°$, scattering was detected by accumulating several 50-point runs at the higher angles, each run having a counting time per point of 5 min. The resulting five ranges on the $s = (4\pi/) \sin\theta$ scale, together with their total measuring time and their total number of counts at the end of each range, are shown in *Table 1*. The highest absolute statistical error of the scattering function $si(s)$ (cf. equation (4)) is reached at 154 nm^{-1} and amounts to 2.5 electron units per average atom and nanometre. The entire curve has been constructed by smoothly linking the ranges after scaling the intensities with factors computed for five-point overlapping regions and differing from unity by no more than 2%.

* To whom correspondence should be addressed

0032-3861/91/091566-08

Table 1 Angular ranges (s scale), total counting time and total number of counts for the measured PAN raw intensity

s (nm^{-1})	0.3–90	90–109	109–126	126–141	141–154
t_{tot} (min)	5	25	60	120	60
N_{tot}[a]	6.7×10^4	2.7×10^5	6.6×10^5	1.5×10^6	1.1×10^6

[a]At the wide-angle side of each range

Parasitic scattering was measured separately with an empty holder arrangement and a statistical accuracy better than $N^{-1/2} = 0.05$.

ANALYSIS OF DATA

The raw scattering data of the sample were corrected according to the formula:

$$I^{corr}(\theta) = \frac{[I_{raw}(\theta) - aI_p(\theta)e^{-(\mu t)_s/\cos\theta}]\, e^{[(\mu t)_s - (\mu t)_f]/\cos\theta}}{(1 + B\theta)[1 + 1.935\cos^2\theta(\cos^2\theta - 1)]} \quad (1)$$

with

$$(\mu t)_s = -\ln(\tau_s) \qquad (\mu t)_f = -\ln(\tau_f) \quad (2)$$

and

$$B = 0.0775(\rho/\text{g cm}^{-3})^{1/2}/\theta_{max} \quad (3)$$

The factor a in equation (1) scales the parasitic scattering to the primary beam level of the sample measurement, and the square bracketed term in the denominator is the polarization factor for the LiF crystal ((2 0 0) plane). The remaining term in the denominator with B from equation (3) is a rough estimate for multiple scattering, based on the Monte Carlo simulations of Pitkänen[9,10]. In equation (2) τ_s and τ_f are the measured transmissions of sample and foils, respectively, the latter being in fact unity for our thin foils.

In $si(s)$, $I^{corr}(\theta)$ has been smoothly extrapolated to $s = 0$ below $\theta = 1.9°$, assuming a parabolic shape and an appropriate $I^{corr}(\theta = 0)$ level. The experimental values at $\theta = 1°$, 1.3° and 1.6° had to be omitted due to primary beam effects. Coherent theoretical structure-independent intensities I^{coh} have been calculated with the analytical fit for the atomic scattering factors f_i (i = C, N, H) given in the *International Tables* (ref. 11, p. 99 (and p. 149 for dispersion corrections)), while the incoherent scattering I^{inc} has been treated according to Hajdu and Pálinkás[12] using a fit proposed by Hajdu[13].

Now the scattering function can be defined as[14]:

$$si(s) = s\frac{cI^{corr}(s) - I^{coh}(s) - I^{inc}(s)}{(\sum_i x_i f_i)^2} \quad (4)$$

with mole fractions x_i ($x_C = x_H = 3/7$, $x_N = 1/7$ for PAN) and the normalization factor c, bringing experimental and theoretical intensities on the same scale, namely electron units squared per average atom. The factor c has been determined both by fitting the high-angle regions and by the method of Krogh-Moe and Norman[15,16]. An optimization of the sample's transmission τ_s has been performed by a procedure similar to that proposed by Ergun[17]. Lowering the measured transmission factor by 4%, agreement between the two normalization factors of 0.03% was obtained in the present case.

The resulting unsmoothed scattering function and its

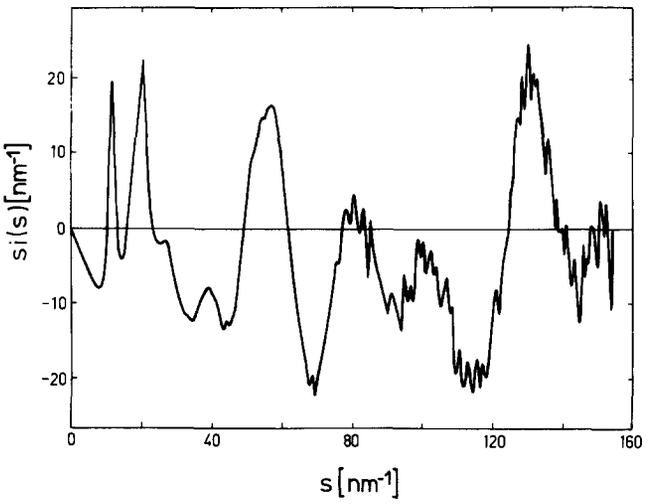

Figure 1 Experimental scattering function $si(s)$ for commercial PAN homopolymer

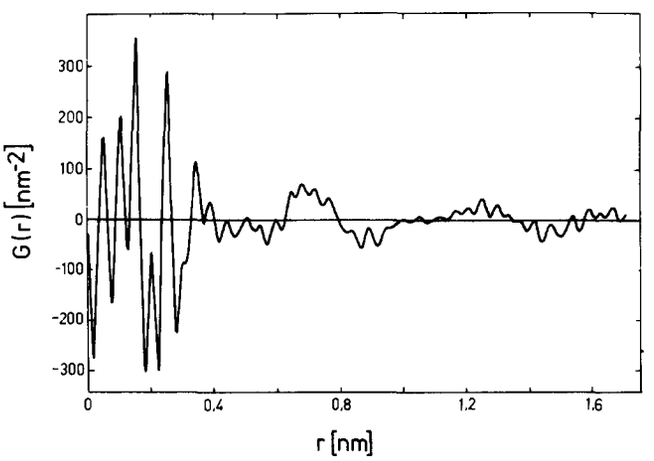

Figure 2 Fourier sine transform $G(r)$ of the function in *Figure 1*

Fourier sine transform:

$$G(r) = \frac{2}{\pi}\int_0^{s_{max}} si(s)\sin(sr)\,ds \quad (5)$$

are shown in *Figures 1* and *2*, respectively. For comparison with model curves (cf. *Figure 10*), the experimental data have been smoothed (running averages) and corrected for erroneous long-wave s oscillations[18].

SINGLE-CHAIN MODELS

Planar zigzag chain (α)

The first model considered here corresponds to the all-*trans* planar zigzag conformation. The only random element for that kind of chain is the tacticity of having the nitrile group below or above the plane defined by the backbone. For PAN, radically polymerized in solution,

n.m.r. investigations show[4] that the tacticity is governed by Bernoullian statistics with equal probability of events 'above' or 'below'. This fact must be taken into account also for the other PAN model chains (β) and (γ), because the tacticity is determined by the polymerization process.

PCILO chain (β)

The second model is based on recent quantum-chemical conformational energy calculations for acrylonitrile diads (2,4-dicyanopentane) carried out with the PCILO method[19]. The local minima found for the *meso-* (*Figure 3a*) and the racemic (*Figure 3b*) diads are shown in *Tables 2* and *3*, together with energy differences to the *trans* conformations, for which the angles ϕ_1 and ϕ_2 (*Figure 3*), counted positive for right-hand rotations, are zero. Molecular symmetry produces further minima $\bar{m}_i$ and $\bar{r}_i$ at $\phi_1(\bar{m}_i) = -\phi_2(m_i)$, $\phi_2(\bar{m}_i) = -\phi_1(m_i)$ and $\phi_1(\bar{r}_i) = \phi_2(r_i)$, $\phi_2(\bar{r}_i) = \phi_1(r_i)$, which have the same energy as m_i and r_i, respectively.

For generating longer PCILO chains, first a tacticity sequence $T(n)$, $n = 1, \ldots, n_{max}$, has been generated with $T(n) = 0$ or 1 if the nth monomer is determined to be added in *meso-* or racemic position with probabilities of 0.5 (cf. subsection (α) above) and arbitrarily fixed $T(1) = 0$. Then n_{max} monomers have been linked in appropriate PCILO minimum positions, taking into account steric hindrance by van der Waals radii R_i with R_C(main chain) = 0.15 nm, R_C(nitrile group) = 0.145 nm, $R_H = 0.095$ nm and $R_N = 0.13$ nm (cf. ref. 20).

The minima used to link the monomers were m_1, $\bar{m}_1$, r_1 and r_2 because of their highest probability at room temperature (Boltzmann statistics). The minima m_2 and $\bar{m}_2$ had to be included to avoid steric hindrance of longer *meso* sequences.

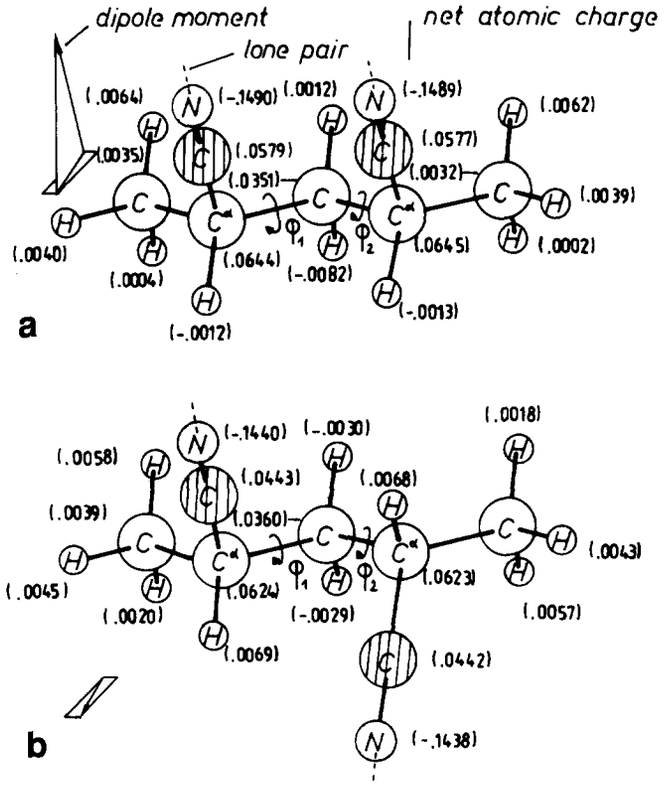

Figure 3 Acrylonitrile diads in (a) *meso-* (*meso*-2,4-dicyanopentane) and (b) racemic (racemic 2,4-dicyanopentane) forms[19]

Table 2 PCILO calculated local conformational energy minima for *meso*-2,4-dicyanopentane and energy differences relative to the *trans* conformation according to ref. 19

Conformation[a]	Abbreviation	(ϕ_1, ϕ_2) (deg)	ΔE (kJ mol^{-1})
$(g^-t)_+$	m_1	(−82.5, −27.5)	−28.5
$(g^-t)_-$	m_2	(−111, −17)	−11.0
tg^-	m_3	(−8, −107)	−7.0
$(g^-g^-)_+$	m_4	(−102, −87)	−2.0
$(g^-g^-)_-$	m_5	(−133, −119)	1.5

[a]Notation from ref. 19

Table 3 Same as *Table 2* for racemic 2,4-dicyanopentane

Conformation[a]	Abbreviation	(ϕ_1, ϕ_2) (deg)	ΔE (kJ mol^{-1})
$(tt)_-$	r_1	(−32.5, −32.5)	−20.3
g^-g^-	r_2	(−87.5, −87.5)	−16.2
g^+t	r_3	(117, 20)	2.3
g^+g^+	r_4	(106, 106)	7.3

[a]Notation from ref. 19

Table 4 Probability for conformation $\mathscr{R}_n$ in the PCILO chain if $\mathscr{R}_{n-1}$ is given, $T(n+1) = 0$ and $\sum_{n'=1}^{n-1} T(n') =$ even

	$\mathscr{R}_{n-1}$				
$\mathscr{R}_n$	m_1	$\bar{m}_1$	m_2	r_1	r_2
m_1	0	0	1	1	0
m_2	1	0	0	0	0
r_1	1	1	1	1	1

Table 5 Probability for conformation $\mathscr{R}_n$ in the PCILO chain if $\mathscr{R}_{n-1}$ is given, $T(n+1) = 1$ and $\sum_{n'=1}^{n-1} T(n') =$ even

	$\mathscr{R}_{n-1}$				
$\mathscr{R}_n$	m_1	$\bar{m}_1$	m_2	r_1	r_2
m_1	0	0	1/2	1/2	0
$\bar{m}_1$	1	0	1/2	1/2	0
r_1	1	1	5/6	5/6	1
r_2	0	0	1/6	1/6	0

An unhindered growth in the range of interest is guaranteed by consideration of the rules given in *Tables 4* and *5*. These tables determine the probability that the nth monomer is linked in conformation $\mathscr{R}_n$ if the conformation of the $(n-1)$st monomer is $\mathscr{R}_{n-1}$ and the tacticity of the $(n+1)$st one is $T(n+1)$. A further parameter is $\sum T(n')$, $n' = 1, \ldots, n-1$, the number of racemic diads up to $n-1$. If this parameter is odd, m_i and $\bar{m}_i$ must be exchanged, for both $\mathscr{R}_n$ and $\mathscr{R}_{n-1}$. The minimum m_1 ($\bar{m}_1$) was used, whenever this was sterically possible. The fractions 1/2 and 5/6, 1/6 occur due to the equal energy of m_1 and $\bar{m}_1$ (when both are sterically allowed) and the ratio of Boltzmann exponentials of r_2 and r_1 of 0.2 at room temperature.

A perspective drawing of a 12-monomer chain, generated according to the rules given above and with conformation $m_1 r_1 \bar{m}_1 \bar{m}_2 \bar{m}_1 r_1 \bar{m}_1 \bar{m}_2 \bar{m}_1 r_1$, together with front (above), top (below) and side (left) views, is shown in *Figure 4*. One unit on the frames around the projections corresponds to 0.01 nm.

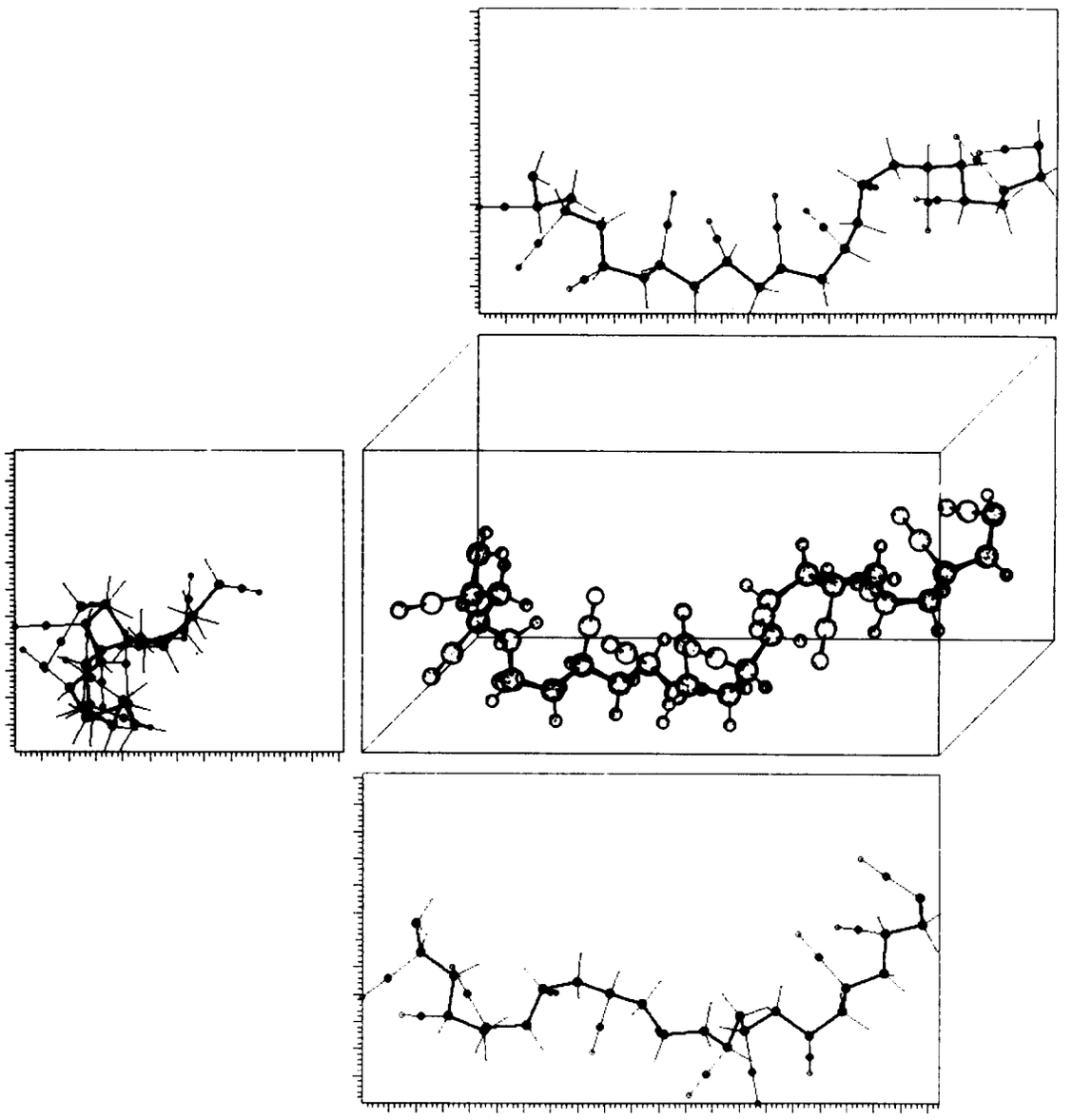

Figure 4 Perspective drawing of a PCILO chain with front (above), top (below) and side (left) views (one unit corresponds to 0.01 nm)

It should be noted that the PCILO calculations predict an attraction of adjacent nitrile groups, in contrast to what one would think[21]. This is due to an increase of nitrogen electronegativity, stabilizing the molecule in the minimum positions through an additional electrostatic energy contribution[19].

Restricted-rotation chain (γ)

The highest degree of disorder is considered in the third kind of model chain, the restricted-rotation chain. With fixed bond lengths and bond angles, all torsional angles along the backbone are allowed with equal probability. Only those are excluded for which any two non-bonded atomic centres have distances less than the sum of the van der Waals radii (see above subsection (β)) of the atoms.

MODEL FUNCTIONS

For the three kinds of model chains described above, reduced radial distribution functions $4\pi r^2[\rho(r)-\rho_0]$ were calculated according to the method proposed by Waring *et al.*[22], employing several chain lengths and averaging procedures. The parameters involved in the Waring method have been chosen to be $\sigma_0 = 0.003$ nm, $\sigma_1 = 0.01$, $\sigma_0^{SAXS} = 0.003$ nm and $\sigma_1^{SAXS} = 0.08$. Scattering functions were obtained through inversion of equation (5) with $s_{max} = \infty$:

$$si(s) = \int_0^\infty G(r)\sin(sr)\,dr \qquad (6)$$

with $G(r) = 4\pi r[\rho(r)-\rho_0]$. In fact, the upper limit of integration can be written as infinity, because $G(r)$ was always (except once) effectively zero above the value actually chosen (2 nm in most cases). For reasons to be discussed later, emphasis is put on scattering functions and only these will be considered in this section.

Planar zigzag chain (α)

In *Figure 5* are shown model scattering functions $si(s)$ for planar zigzag chains of variable length. Curve (a) belongs to a single acrylonitrile monomer, while (b), (c) and (d) are averaged scattering functions for diads, triads and tetrads, respectively. For each of these chain lengths,

G functions for all possible tacticity sequences have been calculated, added, rescaled and transformed. Curve (e) originates from a single planar zigzag chain comprising 120 monomers (120-ad). It is the only one for which the upper limit of Fourier integration was not effectively infinity, so that $si(s)$ is affected by truncation.

Already for the diads (curve (b)) three peaks between $s = 70$ and 110 nm^{-1} occur, which turn out to be typical for the *trans* sequences (curves (c), (d) and (e)). With increasing chain length, peaks evolve at 30, 40 and 150 nm^{-1}.

PCILO chain (β)

Also for the PCILO chain, short sequences have been investigated employing an averaging procedure. For the calculation of averaged scattering functions for diads, triads and tetrads, some sequences of 10000 random conformations have been generated according to the rules given in *Tables 4* and *5*. Then it was found which diads, triads and tetrads occur in these sequences and how often they appear. There are six, 15 and 37 different diads, triads and tetrads, the most frequently occurring three, five and seven of which give 90, 69 and 37% of the total number ($\approx$10000). The remaining three, 10 and 30 diads, triads and tetrads occur with a frequency of less than 4.5% each. Similar to the planar zigzag case (α), scattering functions of the most frequently occurring diads, triads and tetrads have been calculated using weights found in the 10000 sequence leading to the curves (b), (c) and (d) in *Figure 6*. For completeness the monomer scattering (a) has been included.

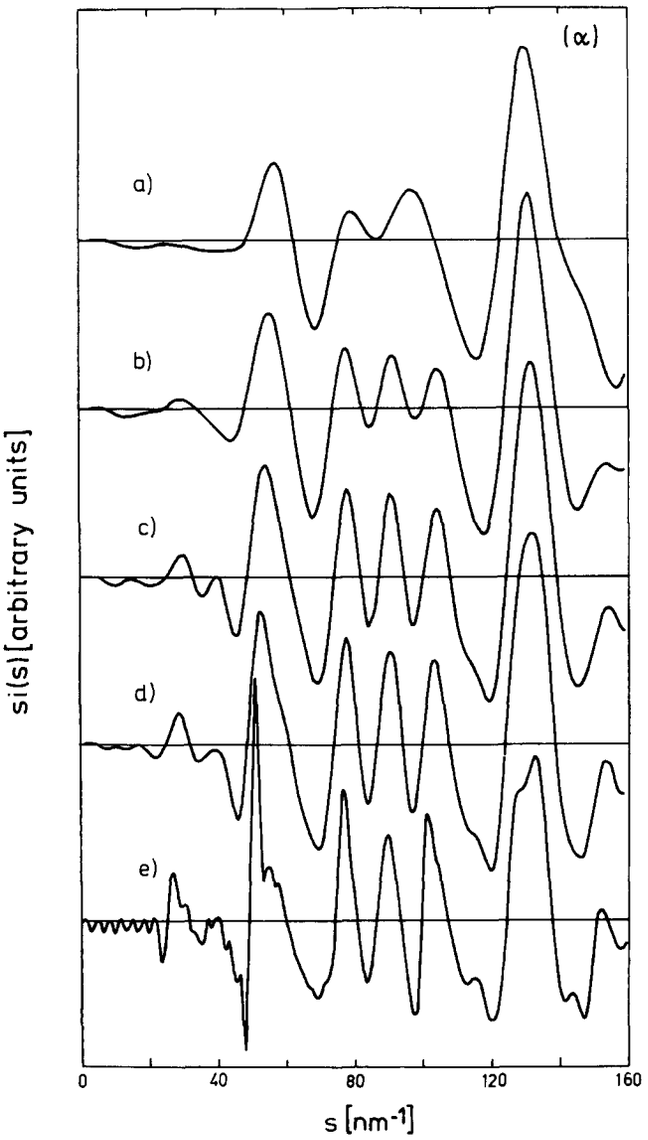

Figure 5 Model scattering functions for planar zigzag conformations (α): (a) monomer; (b), (c) and (d) averaged diads, triads and tetrads; (e) single chain comprising 120 monomers (120-ad)

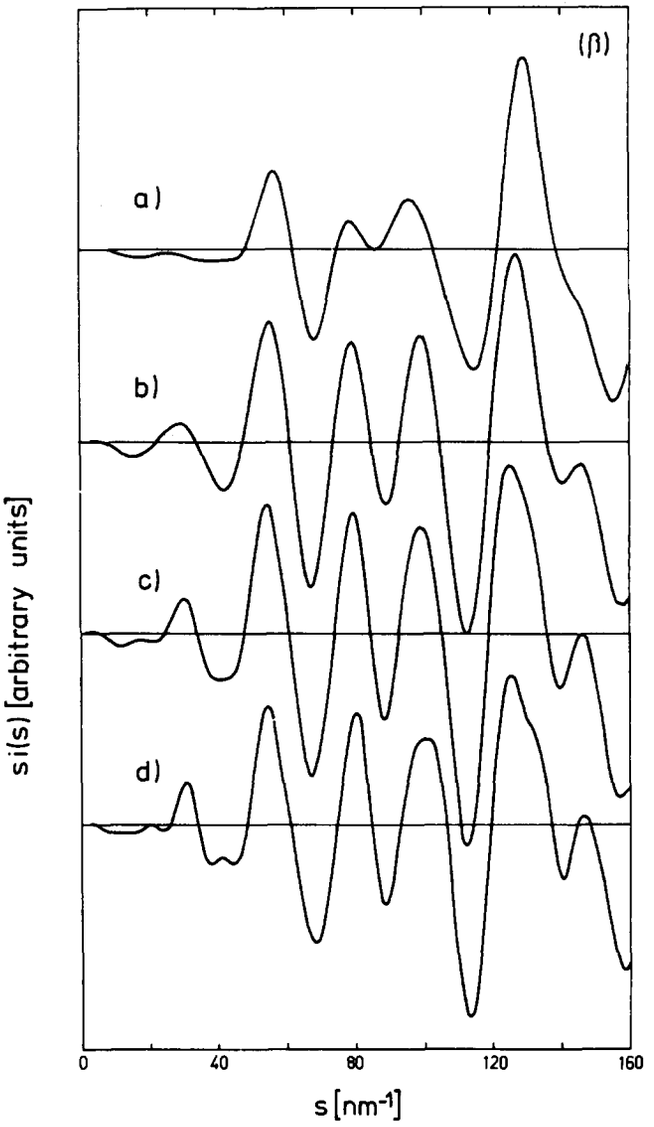

Figure 6 Model scattering functions for PCILO chains (β): (a) monomer; (b), (c) and (d) averaged diads, triads and tetrads

As in the case (α), peaks at 30, 40 and 150 nm^{-1} evolve, but in a slightly different manner. There are only two peaks in the region between 70 and 110 nm^{-1}, rather exactly at 80 and 100 nm^{-1}. The peak at 130 nm^{-1} is slightly shifted left and a shoulder develops on the right side, which is more pronounced for longer sequences, as shown in *Figure 7*. Here the scattering functions of an arbitrarily chosen 12-ad (curve (a)), an averaged one for ten 12-ads (curve (b)) and a 120-ad (curve (c)) are depicted. There is not much difference between the three, indicating that most features of the PCILO chain that can become visible in $si(s)$ curves up to 160 nm^{-1} are indeed brought out and statistical fluctuations have almost cancelled already for the 12-ad. This has been confirmed also for other 12- and 120-ads, not shown here.

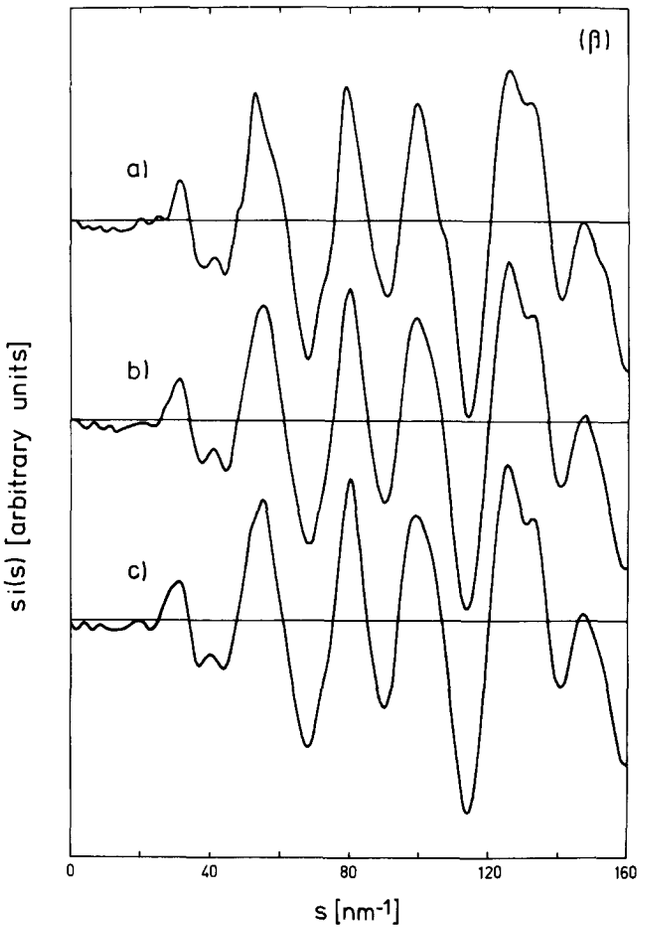

Figure 7 Model scattering functions for PCILO chains (β): (a) 12-ad; (b) averaged 12-ads; and (c) 120-ad

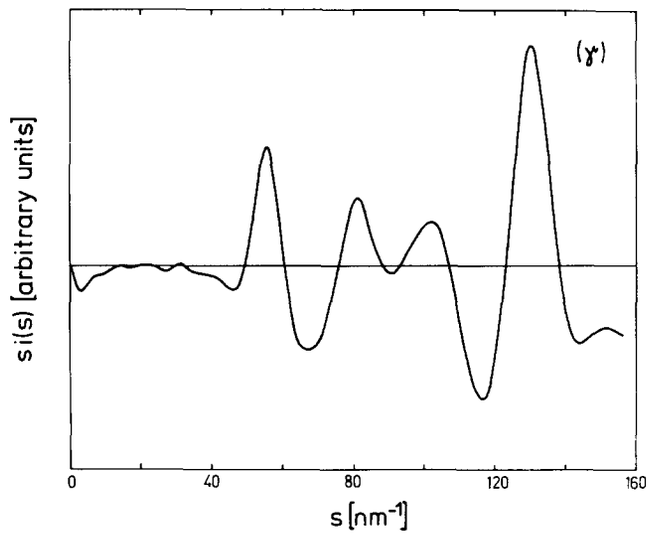

Figure 8 Model scattering function for restricted-rotation chain (γ)

Restricted-rotation chain (γ)

As should be expected for the restricted-rotation chain, the statistical fluctuations are strong, i.e. scattering functions for different rather short random chains look different. Because chain length was limited for computational reasons, 25 $si(s)$ curves for randomly generated 120-ads have been averaged, resulting in the scattering function of *Figure 8*. An average of 20 curves is visually indistinguishable from *Figure 8*, so that 25 120-ads is considered to be sufficient to compensate for the too short chains.

DISCUSSION

First the situation in r space will be discussed with the help of *Figure 9*. In this figure, the experimental $G(r)$ (below) from *Figure 2* is compared with model curves of averaged *trans* tetrads (α), PCILO tetrads (β) and the restricted-rotation chain (γ) from *Figure 8*. These model $G(r)$ functions were calculated from the model $si(s)$ functions truncated at the experimental s_{max}, in contrast to (α'), the *trans*- tetrad function directly calculated from the model.

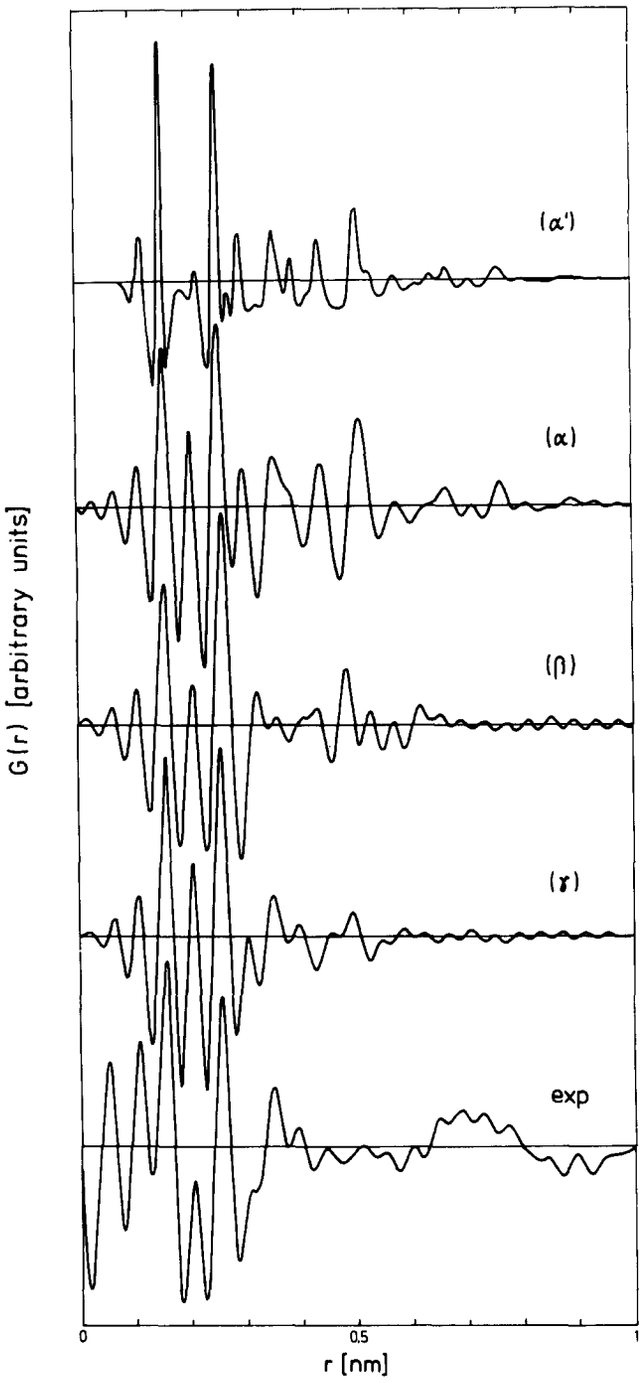

Figure 9 Model ((α')–(γ)) and experimental (exp.) $G(r)$ functions: (α') averaged *trans* tetrads without truncation effect; (α) averaged *trans* tetrads; (β) averaged PCILO tetrads; (γ) restricted-rotation chain

The three peaks at 0.11, 0.15 and 0.25 nm in all the functions are due to C–H nearest-neighbour (0.109 nm), C≡N nitrile group (0.116 nm), C–C nearest-neighbour (0.154 nm) and C–C next-nearest-neighbour (0.252 nm) distances. There is a broadening and a slight shift to the right for the 0.25 nm peak in the PCILO chain curve (β), which is caused by repeated nearest-neighbour nitrile group distances greater than 0.25 nm.

Two reasons can be mentioned for the incomplete match of peak-height ratios. First, the erroneous features visible below 0.1 nm in the experimental curve can also influence the higher r region and produce termination peaks under the real peaks. Secondly, the subtraction procedure for shape scattering involved in the Waring method[22] may not be fully satisfactory in this r range. The sharp peak at 0.2 nm is affected by truncation, as indicated by curve (α') or by comparison with $G(r)$ of a dumped experimental $si(s)$.

Between 0.25 and 0.45 nm only model (γ) matches the experimental curve with some certainty. Above that range no agreement is found and the correlations above 0.8 nm die out for the chains with statistical conformations (γ) and (β). A Fourier transformation of the experimental $si(s)$ curve truncated at 28 nm^{-1}, thus comprising only the two relatively sharp peaks at 12 and 20 nm^{-1}, shows that the broad peak between 0.6 and 0.8 nm and most other features above 0.8 nm in the experimental $G(r)$ are mainly due to these chain packing peaks[23], not being of particular interest in the present work. But already the range between 0.3 and 0.6 nm can be slightly influenced by interchain distances because the transform of the sharp chain packing peaks spreads over the whole r range considered (up to $r_{max} = 3$ nm).

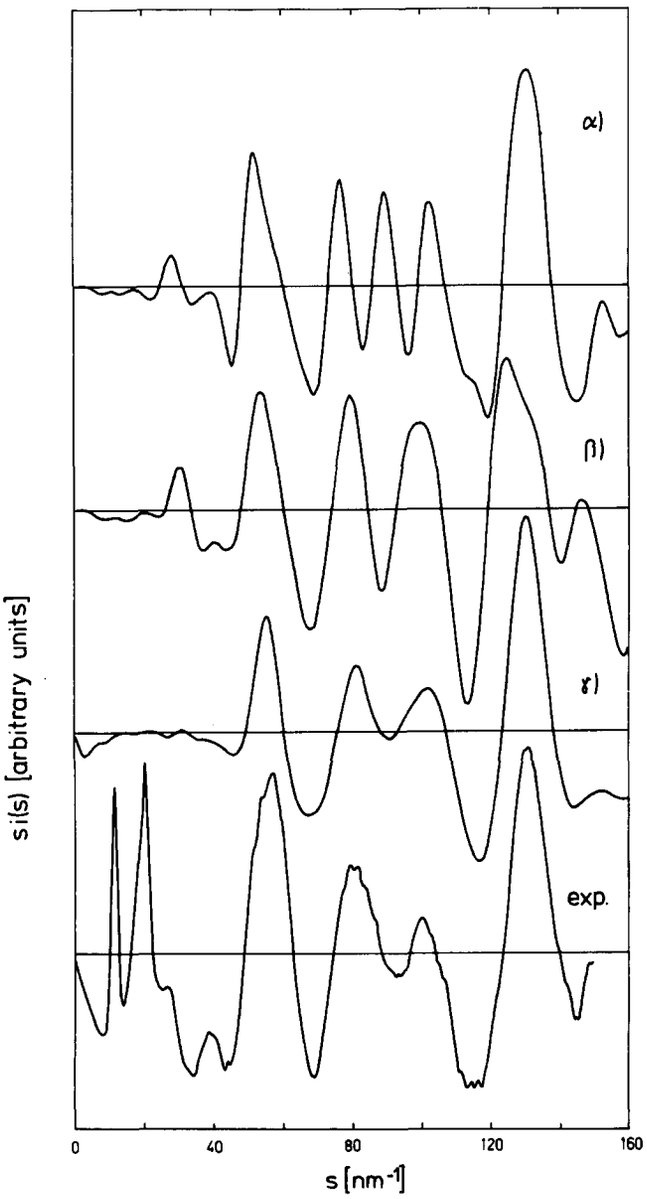

Figure 10 Model ((α)–(γ)) and experimental (exp.) $si(s)$ functions: (a) averaged *trans* tetrads; (β) averaged PCILO tetrads; (γ) restricted-rotation chain

The situation in s space is the opposite. Long-wave s oscillations are produced by the well defined intrachain distances and, additionally, the experimental curve is not affected by truncation. In *Figure 10* model scattering functions $si(s)$ for the averaged *trans* (α) and PCILO (β) tetrad chains, the restricted-rotation chain (γ) and the corrected experimental curve (exp.) are compared.

Apparently, inter- and intrachain information is more clearly separated in reciprocal space. Below 30 nm^{-1} in the 'shape scattering range' of the models, the experimental curve is dominated by the interchain packing peaks at 12 and 20 nm^{-1}, and no agreement between model and experiment can be expected. Between 30 and 50 nm^{-1} the measured curve is reproduced best by the PCILO model (β), although interchain interferences seem to have an influence up to 60 nm^{-1}. Note that at least four acrylonitrile monomers were necessary to produce in the model function one feature of the experimental curve, namely the small peak within a broad minimum around 40 nm^{-1} (cf. *Figure 6*). This does not appear with the same clearness for the much more flexible restricted-rotation chain, indicating that in the sample the chains are more rigid and have some kind of conformational persistence length of at least four monomers (about 0.6–0.8 nm, cf. *Figure 4*).

Above 60 nm^{-1} the experimental curve is matched quite well by the restricted-rotation chain scattering function, except above 140 nm^{-1} where the latter almost remains constant and the former, unambiguously ascends, similar to the PCILO curve. This agreement suggests that the energetically favourable single-chain conformations are somewhat distorted by interchain interactions, thus restricting the conformational correlation length to not much more than four monomers.

The *trans* tetrad function (α) is clearly ruled out as an approximation for the experimental curve, as well as the functions for shorter *trans* sequences (*Figure 5*).

CONCLUSIONS

The following picture is in accord with the experimental findings obtained in the present work. Energetically favourable single-chain conformations are characterized by an effective attraction of adjacent nitrile groups. Strong interchain interactions distort these conformations but do not suffice to cancel all conformational regularity. There remains a coupling of conformations with a correlation length of about four monomers (0.6–0.8 nm). The stiffness of the chain is greater than in the restricted-rotation case. The planar zigzag conformation is not preferred in the investigated PAN sample.

ACKNOWLEDGEMENTS

We are greatly indebted to Dr F. Hajdu for providing us with a BASIC version of his RDF program. We thank Dr D. Hofmann for many helpful discussions.

REFERENCES

1 Bohn, C. R., Schaefgen, J. R. and Statton, W. O. *J. Polym. Sci.* 1961, **55**, 531
2 Grobelny, J., Sokół, M. and Turska, E. *Polymer* 1984, **25**, 1415
3 Yamazaki, H., Kajita, S. and Kamide, K. *Polym. J.* 1987, **19**, 995
4 Kamide, K., Yamazaki, H., Okajima, K. and Hikichi, K. *Polym. J.* 1985, **17**, 1233
5 Klug, H. P. and Alexander, L. E. 'X-ray Diffraction Procedures for Polycrystalline and Amorphous Materials', Wiley, New York, 1974
6 Voigt-Martin, I. and Wendorff, J. in 'Encyclopedia of Polymer Science and Engineering', Wiley, New York, 1985, Vol. 1, p. 789
7 Mitchell, G. R. in 'Order in the Amorphous State of Polymers' (Eds S. E. Keinath, R. L. Miller and J. K. Rieke), Plenum Press, New York, 1987, p. 1
8 Herms, G. and Hajdu, F. *J. Appl. Crystallogr.* 1984, **17**, 140
9 Pitkänen, T., Cooper, M. J., Laundy, D. and Holt, R. S. *Nucl. Instrum. Meth.* (*A*) 1987, **257**, 384
10 Pitkänen, T. Report Series in Physics HU-P-248, University of Helsinki
11 'International Tables for X-ray Crystallography', Kynoch Press, Birmingham, 1974, Vol. IV
12 Hajdu, F. and Pálinkás, G. *J. Appl. Crystallogr.* 1972, **5**, 395
13 Hajdu, F. *Acta Crystallogr.* (*A*) 1972, **28**, 250
14 Pings, C. J. and Waser, J. *J. Chem. Phys.* 1968, **48**, 3016
15 Krogh-Moe, J. *Acta Crystallogr.* 1956, **9**, 951
16 Norman, N. *Acta Crystallogr.* 1957, **10**, 370
17 Ergun, S. *Chem. Phys. Carbon* 1968, **3**, 211
18 Kaplow, R., Strong, S. L. and Averbach, B. L. *Phys. Rev.* (*A*) 1965, **138**, 1336
19 Ganster, J. and Lochmann, R. *Polymer* 1990, **31**, 1159
20 Hopfinger, A. J. 'Conformational Properties of Macromolecules', Academic Press, New York, 1973
21 Henrici-Olivé, G. and Olivé, S. *Adv. Polym. Sci.* 1979, **32**, 12
22 Waring, G. R., Lovell, R., Mitchell, G. R. and Windle, A. H. *J. Mater. Sci.* 1982, **17**, 1171
23 Lindenmeyer, P. H. and Hosemann, R. *J. Appl. Phys.* 1963, **34**, 42